This is a post-peer-review, pre-copyedit version of an article published in **2020 IEEE 14th International Conference on Compatibility, Power Electronics and Power Engineering (CPE-POWERENG)**. The final authenticated version is available online at: https://doi.org/10.1109/CPE-POWERENG48600.2020.9161460

Optimized Space-Vector Modulation Schemes for Five-Phase Precision Low-Speed Drives with Minimizing the Stator Current Ripple

Valentin Tomasov
Department of Control Engineering and Robotics
ITMO University
St. Petersburg, Russia
tomasov@ets.ifmo.ru

Aleksander Usoltsev
Department of Control Engineering and Robotics
ITMO University
St. Petersburg, Russia
uaa@ets.ifmo.ru

Denis Vertegel
Department of Control Engineering and Robotics
ITMO University
St. Petersburg, Russia
vertegeldenis@gmail.com

Pawel Szczepankowski
Department of Electrical and Control Engineering
Gdansk University of Technology
Gdansk, Poland
pawel.szczepankowski@pg.edu.pl

Ryszard Strzelecki
Department of Electrical and Control Engineering
Gdansk University of Technology
Gdansk, Poland
profesor1958@gmail.com

Nikolai Poliakov
Department of Control Engineering and Robotics
ITMO University
St. Petersburg, Russia
polyakov.ets.itmo@gmail.com

***Abstract* — One of the main ways to improve the quality of a precision electric drive is minimization of the stator current pulsations generated by the voltage inverter. The solution of this problem can be achieved by using of multiphase inverters, as well as improving control algorithms. This paper considers the influence of the space-vector modulation algorithm with different switching sequences of basic vectors on the stator current pulsations generated by the five-phase voltage inverter.**

Keywords — multiphase electric drive, space-vector modulation, coefficient of variation, precision electric drive, frequency converters

I. INTRODUCTION

At the present time higher demands are placed on the precision electric drive of modern optical-mechanical complexes to ensure unique pointing accuracy over a wide range of speed control under conditions of variable load. In this regard, such systems are built on the basis of gearless synchronous motors with excitation from permanent magnets. This approach can significantly reduce the amount of Coulomb friction and eliminate the backlash of gears, providing the ability to control the coordinates of movement in a wide range. At the same time, when designing a precision electric drive, it is important to take into account the pulse mode of operation of the voltage inverter, since it leads to the generation of additional pulsations of the electromagnetic torque, which complicates the control process and reduces the accuracy of the entire system [1-3, 7].

By employing a higher number of phases, one can reduce the amplitude and increase the frequency of torque pulsations in the drive. This ensures satisfactory performance of the mechanical system of the inverter-fed motor even at lower speeds. It has also been established that the electrical efficiency of the inverter-fed multiphase motors are better compared to that of a three-phase motor. Increasing the phase numbers will also improve the reliability since the drive can start and run even after the failure of one of the phases [7]. Moreover, in such drives the current load per phase and current pulsations in the DC link are decreased [4].

With the increase of the number of phases, it becomes possible to control independently several harmonics of the stator current that provides the increase of the developed torque of the electric drive under the condition of a trapezoidal distribution of stator flux linkage in the gap [8-10].

Another feature of multiphase systems is associated with the so-called multi-motor drives, which implies the independent control of several multiphase machines with series or parallel connected stator windings using a single multiphase inverter [4, 5, 10-12].

To minimize pulsations of the generated stator current vector and, as a result, pulsations of the electromagnetic torque, it is proposed to consider the possibility of using multiphase voltage inverters in a precision electric drive. In this connection, the study of pulsations associated with the algorithm of the inverter in the mode of spatial-vector modulation is of interest, since it is possible to change the sequence of the base vectors formation, affecting the current and torque pulsations [3].

The paper addresses the above problem and compares PWM modulation schemes in terms of the stator current pulsation. Thus, the aim of the work is to present the influence of the five-phase voltage inverter operation algorithm on the pulsations of the generated stator current vector.

It is important to note that spectral criteria, for example, THD (total harmonic distortion), which estimates only the effective values of higher harmonics without taking into account the phase spectrum of the pulsations, are usually used to assess the quality of electric energy conversion. However, the main function of the voltage inverters in a variable-frequency drive system is the generation of a circular hodograph of the stator current vector, which is why such criteria are not a correct estimate. In this regard, it is proposed to evaluate the quality of the generated stator current using the coefficient of variation [3]:

$$CV = \frac{\sqrt{\frac{1}{T_1}\int_0^{T_1}\left(|\mathbf{I}|(t) - \overline{|\mathbf{I}|}\right)^2 dt}}{\overline{|\mathbf{I}|}}, \qquad (1)$$

where $\overline{|\mathbf{I}|} = \frac{1}{T_1}\int_0^{T_1} |\mathbf{I}|(t)dt$ – average value of the magnitude of the stator current vector $\mathbf{I}(t)$ for the period of the current fundamental harmonic T_1 in the steady-state operation mode.

II. Five-Phase Inverter

The schematic structure of the *m*-phase voltage inverter is shown in Fig. 1. A multiphase system of independent quantities (currents, voltages, EMF) forms a space whose dimension is equal to the number of phases. Using the Clarke's decoupling transformation,

$$\underline{C}_5 = \frac{2}{5}\begin{bmatrix} 1 & \cos(\varphi) & \cos(2\varphi) & \cos(3\varphi) & \cos(4\varphi) \\ 0 & \sin(\varphi) & \sin(2\varphi) & \sin(3\varphi) & \sin(4\varphi) \\ 1 & \cos(3\varphi) & \cos(6\varphi) & \cos(9\varphi) & \cos(12\varphi) \\ 0 & \sin(3\varphi) & \sin(6\varphi) & \sin(9\varphi) & \sin(12\varphi) \\ 1/2 & 1/2 & 1/2 & 1/2 & 1/2 \end{bmatrix}, \quad (2)$$

where $\varphi = 2\pi/5$, this space for a five number of phases can be divided into two-dimensional subspaces or planes, the number of which is equal to the $(m-1)/2 = 2$ and one-dimensional subspace.

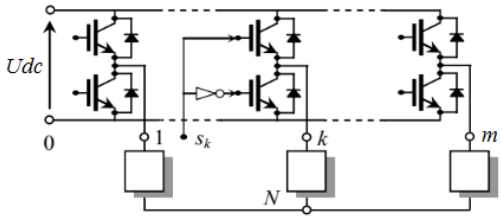

Fig. 1. *m*-phase voltage inverter

For a five-phase system of quantities, this transformation is:

$$\begin{aligned} x_0 &= \frac{1}{5}(y_A + y_B + y_C + y_D + y_E), \\ \mathbf{x}_1 &= \frac{2}{5}(y_A + y_B\boldsymbol{\alpha}^1 + y_C\boldsymbol{\alpha}^2 + y_D\boldsymbol{\alpha}^3 + y_E\boldsymbol{\alpha}^4), \\ \mathbf{x}_2 &= \frac{2}{5}(y_A + y_B\boldsymbol{\alpha}^3 + y_C\boldsymbol{\alpha}^6 + y_D\boldsymbol{\alpha}^9 + y_E\boldsymbol{\alpha}^{12}), \\ \boldsymbol{\alpha} &= e^{j\frac{2\pi}{5}}, \end{aligned} \quad (3)$$

where y_p ($p = \{A, B, C, D, E\}$) is the phase quantity, $\mathbf{x}_1$ is the generalized space vector in the d_1q_1 plane, $\mathbf{x}_2$ is the generalized space vector in the d_2q_2 plane, x_0 is the scalar quantity corresponding to the zero symmetrical component (x_0 is not taken into account in the further work, since in the Y-connected circuit zero symmetric component of the phase currents is zero), $\boldsymbol{\alpha}$ is the rotation operator or the characteristic operator of the five-phase system [4, 6-9, 12-18, 19, 22].

The states of half-bridges of a five-phase inverter (Fig. 1) can be described by a five-digit binary code, assuming, for example, a single value corresponding to the closed state of the upper switch and the open state of the lower. Substituting the digits of this code as the variables y_p in (3), we obtain 32 points on the d_1q_1 and d_2q_2 planes that correspond to the basic vectors (Fig. 2).

As follows from the Fig. 2, a five-phase inverter allows you to generate 30 non-zero (active) and two zero basic vectors (BV) in two planes. In this case, the points of the ends of active BVs form three regular decagons on both planes. Each basic vector is uniquely determined by the combination of states of the inverter power switches, which is indicated by the binary number in Fig. 2. Thus, each plane of the BVs corresponds to a four-level inverter, however, the segments of the sectors have a trapezoidal shape. In this case, the magnitudes of active vectors forming decagons are $S = 0.247U_{dc}$, $M = 0.4U_{dc}$, and $L = 0.647U_{dc}$.

It should be noted that each vector of the d_1q_1 plane corresponds to a vector in the d_2q_2 plane. Moreover, BVs that form the outer decagon in one plane form the inner decagon in the other plane (Fig. 3), while the middle decagons for both planes are formed by identical BVs. In addition, the codirectional vectors of the inner and outer polygons of the d_1q_1 plane remain codirectional in the d_2q_2 plane, but the vectors of the central polygon turns through 180° with respect to them (Fig. 3).

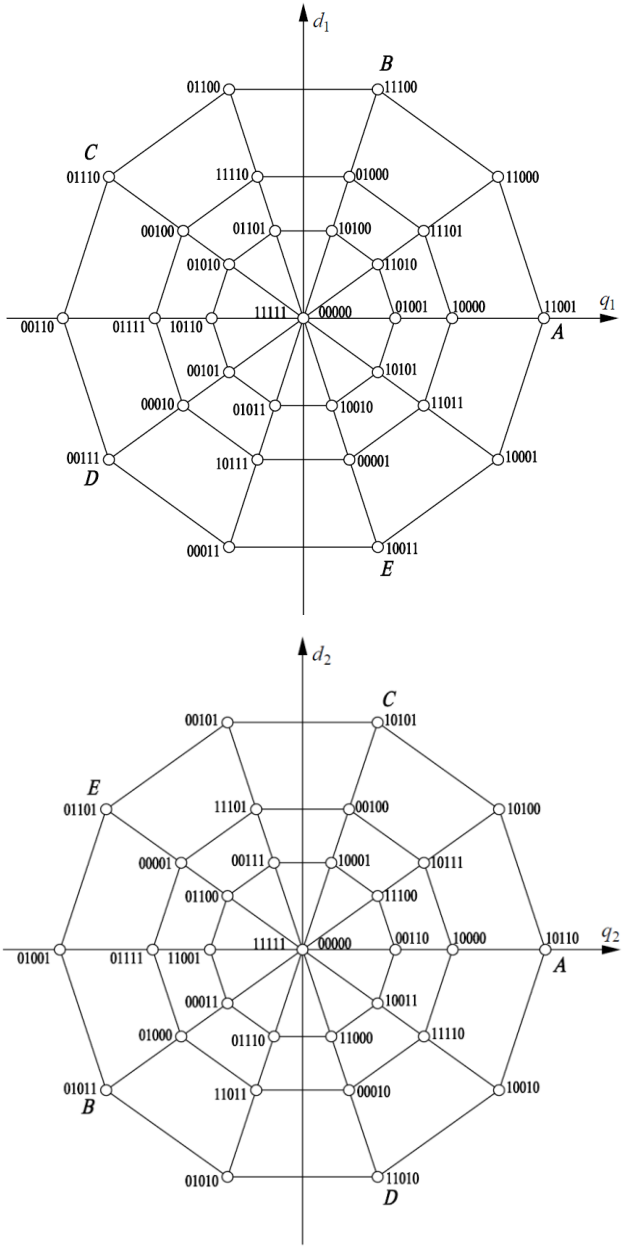

Fig. 2. The planes of the basic vectors of the five-phase inverter

The most important feature of the formation of the BVs in the d_2q_2 plane is a change of the *A-B-C-D-E* phase sequence to *A-C-E-B-D* one (Fig. 2). It means that in case of a sinusoidal distribution of the stator flux linkage of the electric motor, the currents in the d_2q_2 plane do not provide torque and create only leakage fluxes of the stator winding. While in the case of a trapezoidal or square stator flux linkage distribution, the currents in the d_2q_2 plane will create electromagnetic torque [7-10].

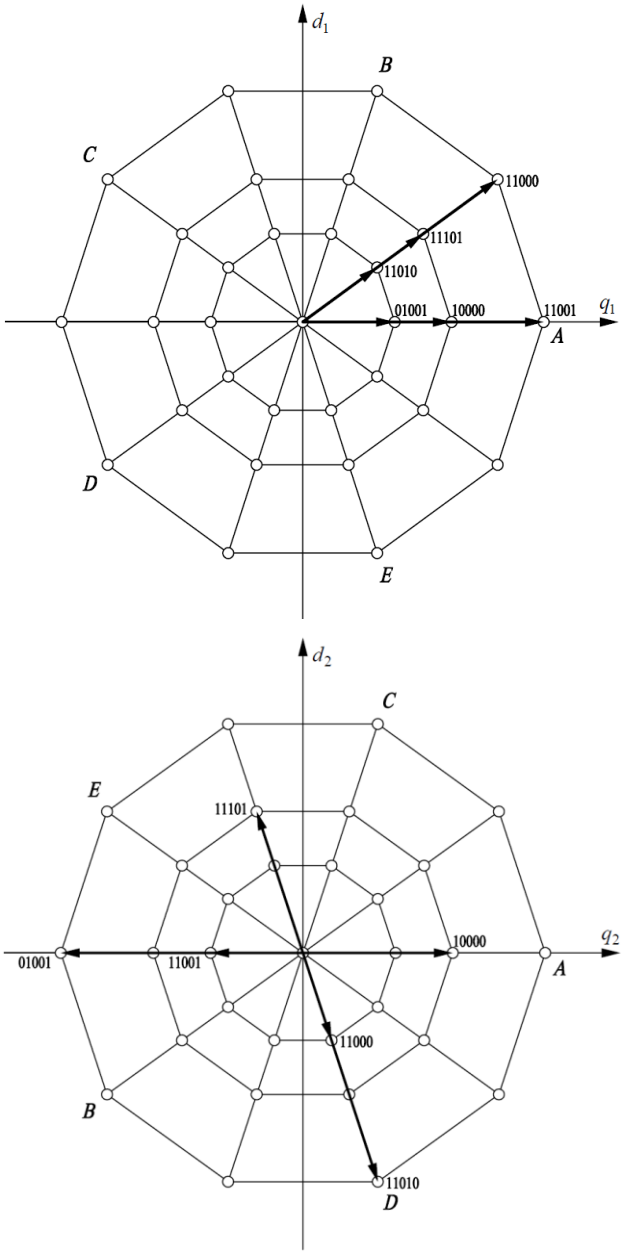

Fig. 3. Correspondence of basic vectors in the d_1q_1 and d_2q_2 planes

III. SVM FOR FIVE-PHASE INVERTER

The implementation of the space-vector modulation (SVM) algorithm is based on the representation of the modulation vector of the inverter output voltage $\mathbf{U}^* = U^* e^{j\vartheta}$ as the average value of the sum of a certain number of BVs generated during the modulation period. The maximum amplitude of the fundamental harmonic of the output voltage in the linear regulation zone in five-phase inverter corresponds to the radius of the circle inscribed in the external decagon, i.e. $U_{1\max} = 0,647 \cdot U_{dc} \cos(18°) \approx 0,616 U_{dc}$, which is almost 7% more than in the three-phase inverter.

The task of implementing the control algorithm can be significantly simplified if we consider only one d_1q_1 plane, forming the modulation vector by the closest BVs. However, this approach will certainly lead to uncontrolled harmonics of current and voltage in the d_2q_2 plane, which, in turn, can cause overheating of the motor windings. In this case, the largest magnitude of the current vector in the d_2q_2 plane will correspond to an algorithm in which only small BVs $\mathbf{S}_1$, $\mathbf{S}_2$ are used (Fig. 4), since in the d_2q_2 plane they correspond to BVs forming an external polygon.

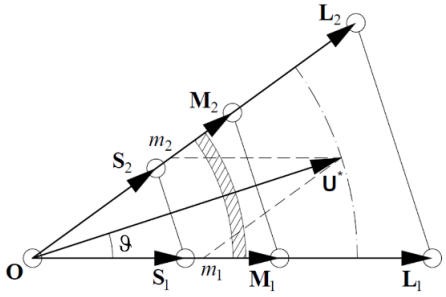

Fig. 4. The first sector of the d_1q_1 plane

There are generally known algorithms that use only zero vector and BVs of the outer decagon closest to the modulation vector (2L), as well as zero vector and BVs of the outer and middle decagon (2L+2M) [6, 14, 15]. In the case of the 2L algorithm, a hodograph is formed on the d_2q_2 plane from a sequence of zero and small BVs, exciting $10k\pm3$ order current harmonics in the load. The 2L+2M algorithm completely eliminates the generation of currents in the d_2q_2 plane, thereby minimizing pulsations. It is possible because the vectors in the d_2q_2 plane corresponding to the vectors bounding the sectors in the d_1q_1 plane have a mutually opposite direction and the same ratio of magnitudes, i.e. $L/M = M/S = 1.618$ (Fig. 3). However, current suppression in the d_2q_2 plane reduces the voltage utilization factor of the DC-link to $0.526U_{dc}$ [6, 14, 15].

The 2L+2M algorithm essentially means the selection in all ten sectors of the d_1q_1 plane of trapezoidal segments corresponding to four BVs. In such a case, as the modulation vector magnitude gets smaller, the active BVs durations decrease, while the zero ones increase, causing an increase of current pulsations. Using the fact that $L/M = M/S$, it is possible to distinguish a second trapezoidal segment formed by medium and small BVs (2M+2S) in each sector. This segment allows to use the same modulation algorithm as in the outer segment, while decreasing the duration of using of the zero BV and, accordingly, current pulsations. We call it the 2L+2M+2S algorithm.

The division of the first sector of the d_1q_1 plane into trapezoidal segments $\mathbf{L}_1\mathbf{L}_2\mathbf{M}_1\mathbf{M}_2$ (LM) and $\mathbf{M}_1\mathbf{M}_2\mathbf{S}_1\mathbf{S}_2$ (MS) is represented in Fig. 4.

The relative duty cycles of the BVs provided that the third harmonic of the phase current for the MS segment is equal to zero can be calculated using the system of equations:

$$\tau_{S1}=\frac{m_1}{u_1+u_3},\qquad \tau_{M1}=\tau_{S1}\frac{u_3}{u_2},$$
$$\tau_{S2}=\frac{m_2}{u_1+u_3},\qquad \tau_{M2}=\tau_{S2}\frac{u_3}{u_2},\qquad (4)$$
$$\tau_O=1-\tau_{S1}-\tau_{S2}-\tau_{M1}-\tau_{M2}.$$

Similarly, for the LM segment, the system of equations is:

$$\tau_{L1}=\frac{m_1}{u_1+u_3},\qquad \tau_{M1}=\tau_{L1}\frac{u_1}{u_2},$$
$$\tau_{L2}=\frac{m_2}{u_1+u_3},\qquad \tau_{M2}=\tau_{L2}\frac{u_1}{u_2},\qquad (5)$$
$$\tau_O=1-\tau_{M1}-\tau_{M2}-\tau_{L1}-\tau_{L2},$$

where τ_i is the relative duty cycles of the corresponding BVs ($i = \{L_1, L_2, M_1, M_2, S_1, S_2, O\}$), $m_1=\left|\mathbf{U}^*\right|[\cos(\vartheta)-\mathrm{ctg}(36°)\sin(\vartheta)]$, $m_2=\left|\mathbf{U}^*\right|\sin(\vartheta)/\sin(36°)$ are the oblique projections of the modulation vector $\mathbf{U}^*$ onto the sector sides, u_1, u_2, u_3 are the magnitudes of the basic vectors equal to 0.247 U_{dc}, 0.4 U_{dc} and 0.647 U_{dc}, respectively, and ϑ is the angle of the modulation vector within the current sector (Fig. 4).

We introduce the definition of the modulation coefficient k_m as the ratio of the modulation vector magnitude to the maximum amplitude of the first voltage harmonic $U_{1\max}$. From the system of equations (5) for the minimum magnitude of the vector $\mathbf{U}^*$ inside the LM segment, the modulation coefficient is 0.561. At the same time, from the (4) the modulation coefficient corresponding to the maximum value of the magnitude of the $\mathbf{U}^*$ in the MS segment is 0.528. Thus, there is a transition zone $0.528 \le k_m \le 0.561$, within which the modulation is carried out alternately in both segments (shaded area in Fig. 4). In addition, the upper limit of the control range for the magnitude of the vector $\mathbf{U}^*$ inside the LM segment is achieved at k_m = 0.854 (dash-dot line in Fig. 4).

It is known that current pulsations depend not only on the algorithm and the modulation frequency, but also on the sequence of the formation of the BVs within the modulation period. It is related to the fact that the change of the switching sequence leads to the change of the initial conditions at each switching, which inevitably leads to the change of the current vector hodograph and, as a consequence, to the change of the pulsations [3].

Due to the fact that in the 2L+2M+2S algorithm five BVs are used during one modulation period T_c, the number of possible switching sequences for each segment is 5! = 120. Obviously, the minimization of the pulsation amplitude of the stator current vector can be achieved by the formation of the switching sequences with the use of the adjacent BVs of the sector. On the other hand, in order to reduce angular pulsations of the stator current vector, the transitions within the sector should be performed with phase alternating (Fig. 5). Thus, there are only seven unique switching sequences, which ensure that these conditions are met. Fig. 6 shows all this sequences for LM segment of the first sector. Similarly, switching sequences are formed for the MS segment.

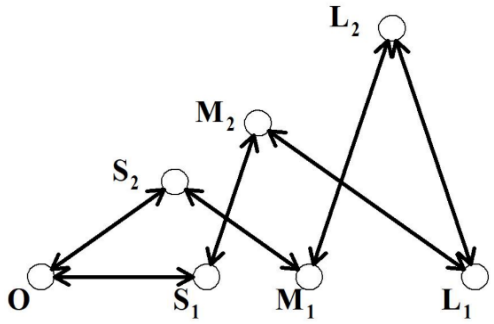

Fig. 5. Admissible transitions between BVs in the first sector of d_1q_1 plane

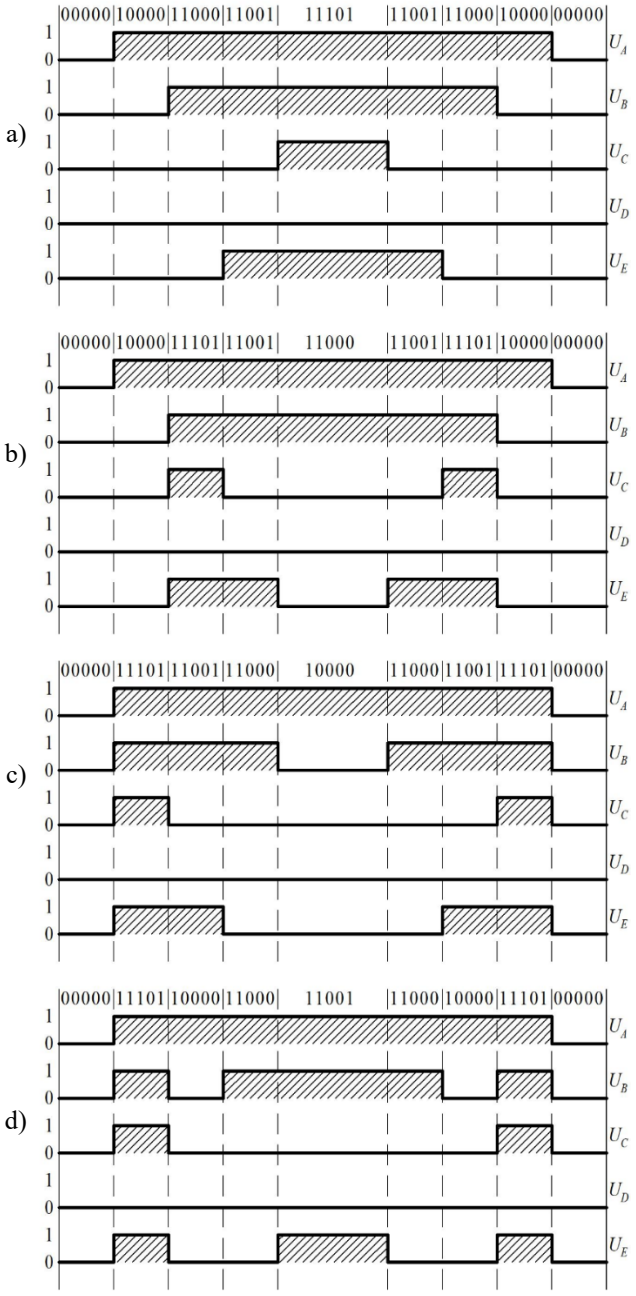

Fig. 6. Switching sequences for the LM segment:
a) – **O-M₁-L₂-L₁-M₂-L₁-L₂-M₁-O**,
b) – **O-M₁-M₂-L₁-L₂-L₁-M₂-M₁-O**,
c) – **O-M₂-L₁-L₂-M₁-L₂-L₁-M₂-O**,
d) – **O-M₂-M₁-L₂-L₁-L₂-M₁-M₂-O**,

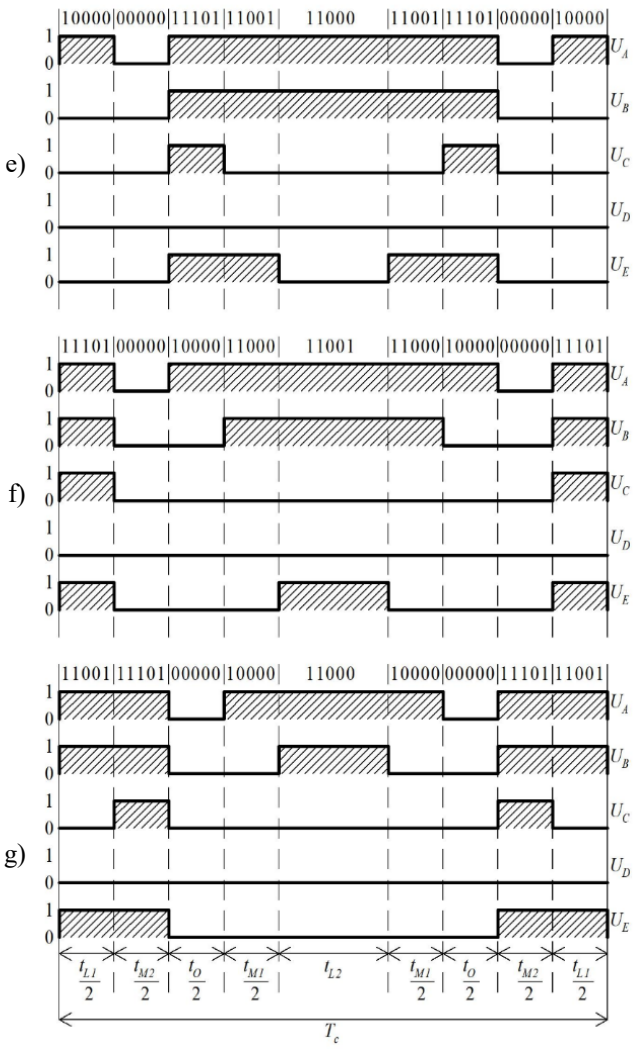

Fig. 6. Switching sequences for the LM segment:
e) – **M₁-O-M₂-L₁-L₂-L₁-M₂-O-M₁**,
f) – **M₂-O-M₁-L₂-L₁-L₂-M₁-O-M₂**,
g) – **L₁-M₂-O-M₁-L₂-M₁-O-M₂-L₁**

IV. Simulation Results

The simulation results of the five-phase inverter with SVM are shown in Fig. 7. The simulation was performed in Matlab/Simulink under the condition U^*/f^*=const (f^* is the rotation frequency of the modulation vector), the modulation frequency f_c =100 f^*, the electromagnetic time constant of the load T_e = 3.25 ms. A symmetrical RL-circuit was used as the inverter load to evaluate the current pulsations, since the passive circuit is sufficient, especially in the low-frequency region, where these pulsations are of the greatest interest and the rotational EMF is almost zero.

Hodographs of the current vectors in the d_1q_1 and d_2q_2 planes at k_m = 0.45 for 2L + 2M algorithm and 2L + 2M + 2S one are shown in Fig. 7a and Fig. 7b respectively. It is seen that in this case the pulsations of the current vector in d_1q_1 plane for 2L+2M algorithm are about twice as much as for 2L+2M+2S algorithm. At the same time, current vectors in the d_2q_2 plane are zero for both algorithms. Fig. 7c shows magnitude of pulsations of the current vector hodographs of the d_1q_1 plane in the time domain.

The value areas of the coefficient of variation for seven considered switching sequences of the proposed 2L+2M+2S algorithm and the 2L+2M one are shown in the Fig. 8. A red line in the Fig. 8 corresponds to the switching sequence of the 2L+2M algorithm [15].

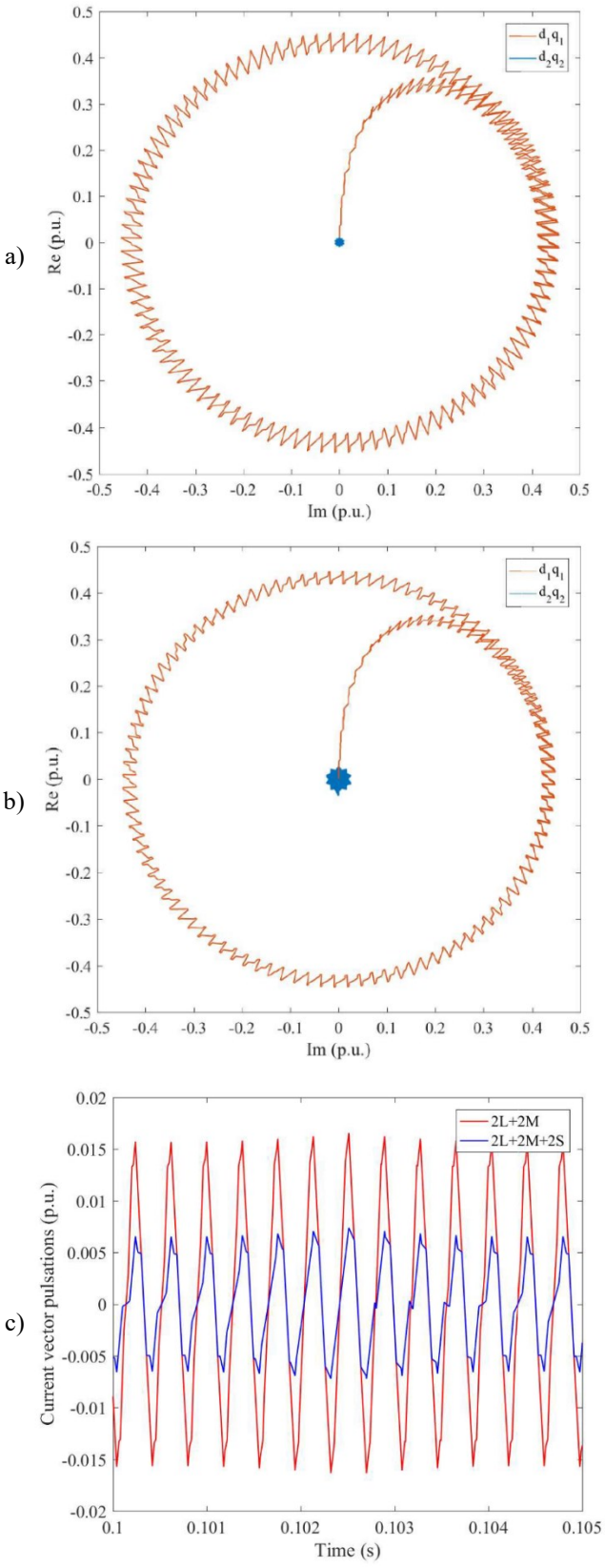

Fig. 7. Hodographs of the current vectors: a – 2L+2M algorithm, b – 2L+2M+2S algorithm; c – magnitude of the current vector pulsations

Obviously, the choice of the switching sequence of the BVs significantly affects the level and power of the current pulsations, especially at low values of k_m, where minimization of pulsations is a high-priority task for the precision electric drives. At low frequencies $f^* < 19\,\text{Hz}$ $(k_m < 0.2)$, by choosing a switching sequence, the level of the CV of the current vector in the d_1q_1 plane can be reduced by about 1.5 times for both algorithms. From the Fig. 8 it also follows that for the 2L+2M+2S algorithm the transition of the modulation vector from one segment to another leads to the violation of the function $\text{CV} = f(\text{k}_m)$ monotony in the area of $0.528 \le k_m \le 0.561$, which requires consideration when designing a precision electric drive, because it can lead to the resonance phenomena.

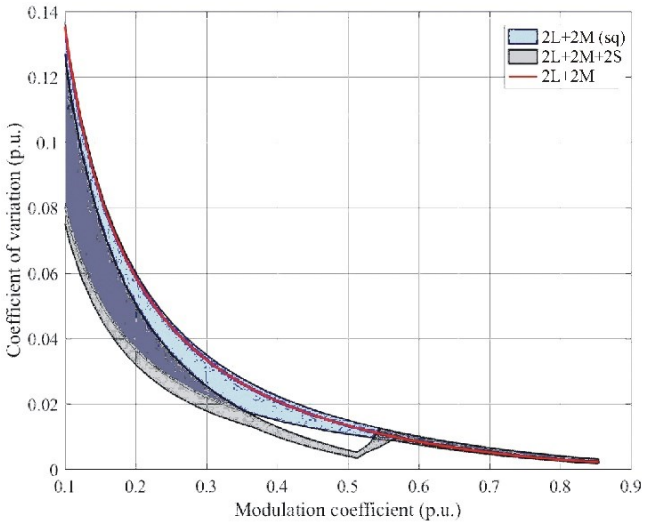

Fig. 8. Coefficient of variation of the stator current

It is important to note that for both algorithms considered (Fig. 8), the lowest CV is achieved by using the sequence shown in Fig 6g, while the worst CV is provided when using the sequence shown in Fig. 6d. Moreover, the upper boundary of the CV region almost corresponds to the 2L+2M algorithm optimized to minimize higher voltage harmonics [15].

V. Conclusion

Thus, the following conclusions can be drawn from the simulation results:

1) when developing a precision electric drive, it is important to consider the modulation algorithm, since changing the switching sequence can significantly reduce the level of the stator current pulsations;

2) the segmentation of the basic vectors plane and the proposed 2L+2M+2S algorithm provide suppression of the low order current harmonics and have the lower CV of the current vector in d_1q_1 plane compared to the 2L+2M algorithm optimized to minimize higher voltage harmonics;

3) a multiphase two-level inverter with the segmentation of the basic vectors plane is actually a multi-level inverter, so the transition from one segment to another results in the sharp change in the magnitude of the current pulsations, what is typical for all multilevel inverters.

References

[1] Tomasov V. S., Usoltsev A. A., Vertegel D. A. Features of using multilevel inverters in precision servo systems. Journal of Instrument Engineering. 2018. Vol. 61, N 12. pp. 1052–1059.

[2] Lovlin S., Abdullin A. Adaptive system for compensation of periodic disturbances in servo drive, 9th International Conference on Power Drives Systems, ICPDS 2016 - Conference Proceedings, IET - 2016, pp. 1–5.

[3] Tomasov V. S., Usoltsev A. A., Vertegel D. A., Strzelecki R. Space vector modulation in multilevel inverters of the servo drives of the trajectory measurements telescopes. Journal of Instrument Engineering. 2017. Vol. 60, N 7. pp. 624–634.

[4] A. Lega, M. Mengoni, G. Serra, A. Tani and L. Zarri, "General theory of space vector modulation for five-phase inverters," IEEE International Symposium on Industrial Electronics. 2008, pp. 237–244.

[5] S.N. Vukosavic,, M. Jones, E. Levi, D. Dujic. Experimental Performance Evaluation of a Five-Phase Parallel-Connected Two-Motor Drive, 4th IET International Conference on Power Electronics, Machines and Drives. 2008 pp. 686–690.

[6] A. Iqbal, E. Levi, Space vector modulation schemes for a five-phase voltage source inverter, 2005 European Conference on Power Electronics and Applications, Dresden, 2005, pp. 1–12.

[7] Levi E., Bojoi R., Profumo F.,Toliyat H., Williamson S.:Multiphase induction motor drives – a technology status review, IET Electr. Power Appl., vol. 1, no. 4, pp. 489–516, 2007.

[8] Mengoni M, Zarri L., Tani A., Parsa L., Serra G.,Casadei D: High-Torque-Density Control of Multiphase Induction Motor Drives Operating Over a Wide Speed Range, IEEE Trans. Ind. Electron., vol. 62, no. 2, pp. 814–825, Feb. 2015.

[9] Kim N.,Baik W. :A five-phase IM vector control system including 3rd current harmonics component," in Power Electronics and ECCE Asia, 2011 IEEE 8th International Conference on, 2011, pp. 2519–2524.

[10] Parsa L.: On advantages of multi-phase machines IECON Proceedings, 2005, pp. 1574–1579.

[11] E. Levi: Multiphase electric machines for variable-speed applications, IEEE Trans. Ind. Electron., vol. 55, no. 5, pp. 1893–1909, 2008.

[12] Iqbal A., Levi E.:Space vector PWM for a five-phase VSI supplying two five-phase series-connected machines, EPE-PEMC, Portoz, Slovenia, 2006, pp. 222–227.

[13] Iqbal A., Moinuddin S., Khan M.: Space Vector Model of A Five-Phase Voltage Source Inverter, 2006, IEEE International Conference on Industrial Technology, 2006, pp. 488–493.

[14] Silva P., Fletcher J., Williams B.: Development of space vector modulation strategies for five phase voltage source inverters, PEMD 2004, vol. 2, p. 650-655 Vol.2.

[15] Iqbal A., Levi E.: Space vector modulation schemes for a five-phase voltage source inverter, European Conference on Power Electronics and Applications, 2005, pp. 1–12.

[16] Ryu H., Kim J., Sul S.: Analysis of multiphase space vector pulse-width modulation based on multiple d-q spaces concept, IEEE Trans. Power Electron., vol. 20, no. 6, pp. 1364–1371, 2005.

[17] Hongwei G., Jianyong S., Guijie Y., Zhao P.: The design of SVPWM IP core for five-phase voltage source inverter,IPEMC 2012, pp. 992–996.

[18] Duran M., Levi E.: Multi-Dimensional Approach to Multi-Phase Space Vector Pulse Width Modulation, IECON 2006, pp. 2103–2108.

[19] Duran F., Toral S., Barrero F., Levi E.: Real-time implementation of multi-dimensional five-phase space vector PWM using look-up table techniques, IECON 2007, pp. 1518–1523.

[20] Gataric S.: A polyphase cartesian vector approach to control of polyphase AC machines IAS 2000, vol. 3, pp. 1648–1654.

[21] Zulkifli M., Munim W. Haris H.:Five Phase Space Vector Modulation Voltage Source Inverter using large vector only," ISCAIE, 2012, pp. 5–9.

[22] Dujic D.,Grandi G.,Jones M.,Levi E.:A space vector PWM scheme for multifrequency output voltage generation with multiphase voltage-source inverters, IEEE Trans. Ind. Electron., vol. 55, no. 5, pp. 1943–1955, 2008.